EDGE ARTICLE

Check for updates

Heterogeneously catalyzed thioether metathesis by a supported Au–Pd alloy nanoparticle design based on Pd ensemble control†

Takehiro Matsuyama, [ID] [a] Takafumi Yatabe, [ID] *[ab] Tomohiro Yabe [ID] [a] and Kazuya Yamaguchi [ID] *[a]

C–S bond metathesis of thioethers has gained attention as a new approach to the late-stage diversification of already existing useful thioethers with molecular frameworks intact. However, direct or indirect thioether metathesis is scarcely reported, and heterogeneously catalyzed systems have not been explored. Here, we develop heterogeneously catalyzed direct thioether metathesis using a supported Au–Pd alloy nanoparticle catalyst with a high Au/Pd ratio. The Au-diluted Pd ensembles suppress the strong π-adsorption of diaryl thioethers on the nanoparticles and promote transmetalation *via* thiolate spill-over onto neighboring Au species, enabling an efficient direct thioether metathesis.

Introduction

Multimetallic nanocatalysts can exhibit higher catalytic performance and/or selectivity than their monometallic counterparts. This high performance is usually attributed to three alloy effects—ensemble, ligand, and strain effects[1]—which are difficult to study in isolation. Nevertheless, according to some reports, the dominant effect is metal ensembles on the nanoparticle surfaces.[1a] The decreased ensembles of active metal species alter the adsorption configuration of molecules[2] or exhibit a single atom-like character,[3] resulting in unique catalytic properties. Such catalyst designs based on ensemble control are uniquely applicable to nanoparticle catalysts and have the potential to realize novel molecular transformations.

Diaryl thioethers are widely used in polymers, natural products, bioactive compounds, and pharmaceuticals.[4a–c] Late-stage diversification of diaryl thioethers, which enables functionalization and transformation of complex molecules without disrupting their building blocks, has therefore become an important goal in synthetic organic chemistry, medicinal science, and materials science.[4] One desirable approach is C–S bond metathesis of diaryl thioethers, which synthesizes novel diaryl thioethers from already existing useful thioethers. The first C–S bond metathesis of diaryl thioethers was reported by Morandi et al.,[5a] who also constructed porous organic polymers

with two- and three-dimensional cores under mild reaction conditions (~80 °C) using a homogeneous Pd complex catalyst.[5b] Theoretically, direct C–S bond metathesis of diaryl thioethers can proceed through the following catalytic cycle: adsorption and oxidative addition of thioethers to Pd species, transmetalation between oxidative adducts, and then reductive elimination and desorption of thioethers from Pd species (Scheme 1a). However, the direct metathesis does not occur in their reports[5a,b] possibly because the transmetalation step is prohibitively difficult on Pd complex catalysts. Thus, thiols and lithium bis(trimethylsilyl)amide are required for their reaction systems: indirect C–S/C–S cross-metathesis *via* C–S/S–H metathesis between diaryl thioethers and thiols (Scheme 1b).[5] Quite recently, Audisio et al. reported Ni-catalyzed direct C–S/C–S cross-metathesis of various thioethers for isotope labelling without using thiols and bases;[6] however, C–S bond metathesis of diaryl thioethers was not demonstrated. On the other hand, recently, we achieved the first example of direct C–S bond metathesis of diaryl thioethers using only Pd acetate and tricyclohexylphosphine (PCy$_3$) as catalyst precursors.[7] The active species of metathesis was confirmed as *in situ*-formed Pd nanoclusters, which likely enable direct crossover between two oxidative adducts (Scheme 1c). However, heterogeneously catalyzed C–S bond metathesis of diaryl thioethers, including indirect metathesis, is demanded for practical use and green sustainable chemistry but has not been attained. In fact, supported monometallic Pd nanoparticles hardly catalyze C–S bond metathesis between phenyl sulfide (**1a**) and *p*-tolyl sulfide (**1b**), even with PCy$_3$ (Table S1†).[7] Clearly, an additional catalyst design is required for heterogeneously catalyzed thioether metathesis.

This study proposes a heterogeneously catalyzed efficient direct C–S bond metathesis of diaryl thioethers using a TiO$_2$-

[a]Department of Applied Chemistry, School of Engineering, The University of Tokyo, 7-3-1 Hongo, Bunkyo-ku, Tokyo 113-8656, Japan. E-mail: kyama@appchem.t.u-tokyo.ac.jp; yatabe@appchem.t.u-tokyo.ac.jp; Fax: +81-3-5841-7220

[b]Precursory Research for Embryonic Science and Technology (PRESTO), Japan Science and Technology Agency (JST), 4-1-8 Honcho, Kawaguchi, Saitama 332-0012, Japan
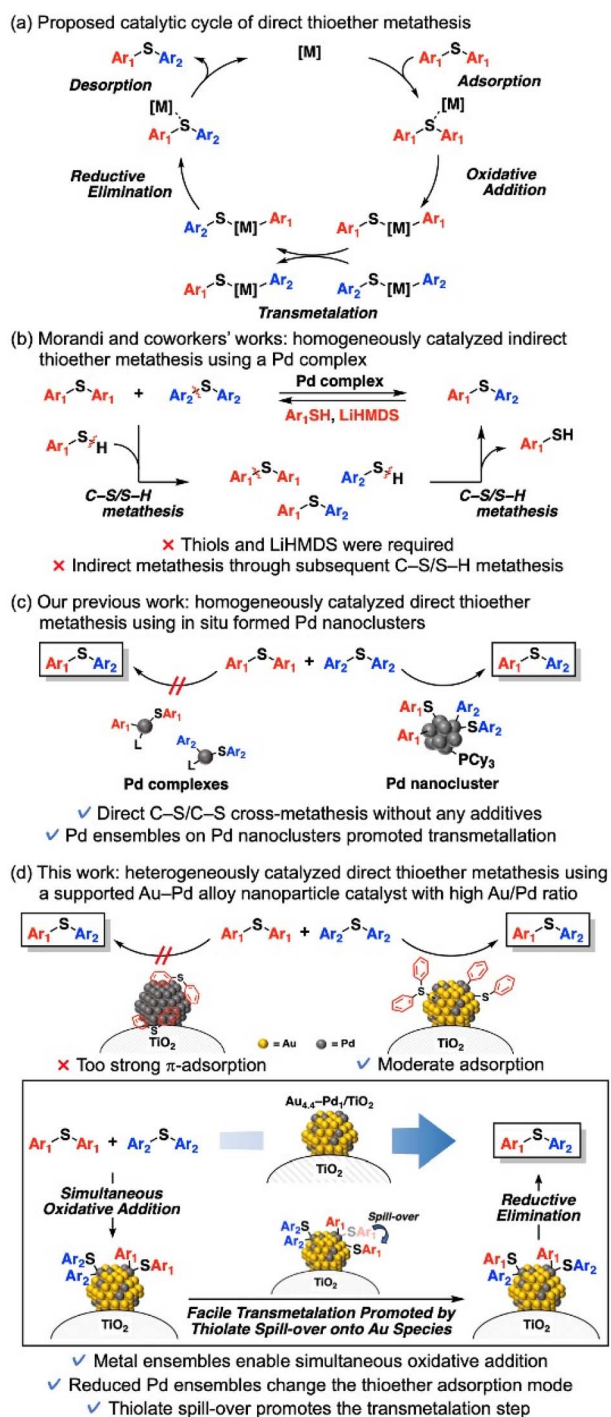
† Electronic supplementary information (ESI) available. See DOI: https://doi.org/10.1039/d4sc02732a

supported Au–Pd alloy nanoparticle catalyst ($Au_{4.4}$–Pd_1/TiO_2) without any additives (Scheme 1d). This catalytic system exhibits a wide substrate scope and functional group tolerance; moreover, the catalyst can be reused a few times. Catalyst characterization and density functional theory (DFT) calculations of cluster models showed that when the Pd ensembles are diluted by Au alloying, the changed adsorption mode of thioethers on the nanoparticles lowers the adsorption/desorption energy and enables C–S bond metathesis. We also suggest that oxidative addition of thioethers produces thiolate species on the Pd species, which migrate to the Au species and promote the transmetalation step, thereby achieving efficient thioether metathesis.

Results and discussion

$Au_{4.4}$–Pd_1/TiO_2 was prepared *via* simultaneous deposition–precipitation of Au and Pd hydroxides (Au/Pd molar ratio = 4.4) on TiO_2, followed by reduction using $NaBH_4$ in deionized water.

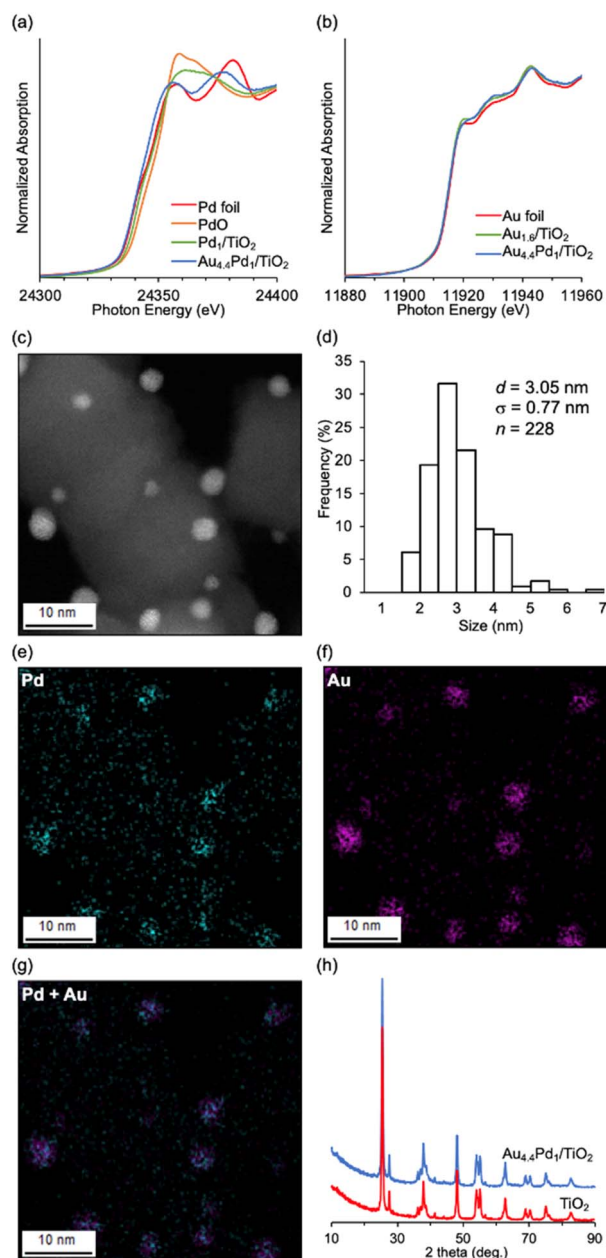Scheme 1 Background (a)–(c) and (d) overview of the present study.

Fig. 1 Characterization of $Au_{4.4}$–Pd_1/TiO_2: (a) Pd K-edge and (b) Au L_{III}-edge XANES spectra and (c) HAADF-STEM image of $Au_{4.4}$–Pd_1/TiO_2; (d) size distribution of nanoparticles on $Au_{4.4}$–Pd_1/TiO_2; (e)–(g) STEM-EDS mappings of $Au_{4.4}$–Pd_1/TiO_2 showing the distributions of Pd [cyan, panel (e)] and Au [magenta, panel (f)]; (g) overlap of (e) and (f); (h) XRD patterns of TiO_2 and $Au_{4.4}$–Pd_1/TiO_2.

The Pd K-edge and Au L_{III}-edge X-ray absorption near edge structure (XANES) spectra of $Au_{4.4}$–Pd_1/TiO_2 were similar to those of Pd foil and Au foil, respectively (Fig. 1a and b), indicating zero valence of Pd and Au, as inferred from the Pd 3d and Au 4f X-ray photoelectron spectra of $Au_{4.4}$–Pd_1/TiO_2 (Fig. S1†). From high-angle annular dark-field-scanning transmission electron microscopy (HAADF-STEM) images, the mean diameter of the TiO_2-supported metal nanoparticles was determined as 3.05 nm ($\sigma = 0.77$ nm; Fig. 1c and d). From the almost coincident locations of Pd and Au species in the STEM-energy-dispersive spectroscopy (EDS) mapping of $Au_{4.4}$–Pd_1/TiO_2 (Fig. 1e–g) and the fitting of the Pd K-edge and Au L_{III}-edge extended X-ray absorption fine structure spectra (indicating that the scatterings originated from Au–Pd bonds; see Fig. S2 and Table S2†), we inferred that Au–Pd alloy nanoparticles were supported on TiO_2. Moreover, the X-ray diffraction (XRD) patterns of $Au_{4.4}$–Pd_1/TiO_2 and TiO_2 were comparable (Fig. 1h), confirming that the TiO_2 structure was unchanged during the catalyst preparation.

Table 1 lists the reaction conditions for investigating the effect of Pd-based supported nanoparticle catalysts on C–S bond metathesis between **1a** and **1b**. A quantitative metathesis can obtain two equivalents of phenyl p-tolyl sulfide (**1ab**) on the basis of **1b**. Based on our previous report,[7] we first investigated a monometallic TiO_2-supported Pd nanoparticle catalyst but **1ab** was hardly obtained (Table 1, entry 1).‡ Among several TiO_2-supported Pd-based bimetallic nanoparticle catalysts, the Au–Pd alloy nanoparticle catalyst exhibited the highest catalytic performance for C–S bond metathesis (Table S3†). We therefore prepared supported Au–Pd alloy nanoparticle catalysts with various Au/Pd ratios (Au_x–Pd_1/TiO_2, x: Au/Pd molar ratio). The catalytic performance of metathesis improved with increasing Au/Pd ratio in the catalyst, reaching a **1ab** yield of 55% for $Au_{4.4}$–Pd_1/TiO_2 (Table 1, entries 2–5). $Au_{1.6}/TiO_2$ hardly catalyzed the reaction and a physical mixture of $Au_{1.6}/TiO_2$ and Pd_1/TiO_2 did
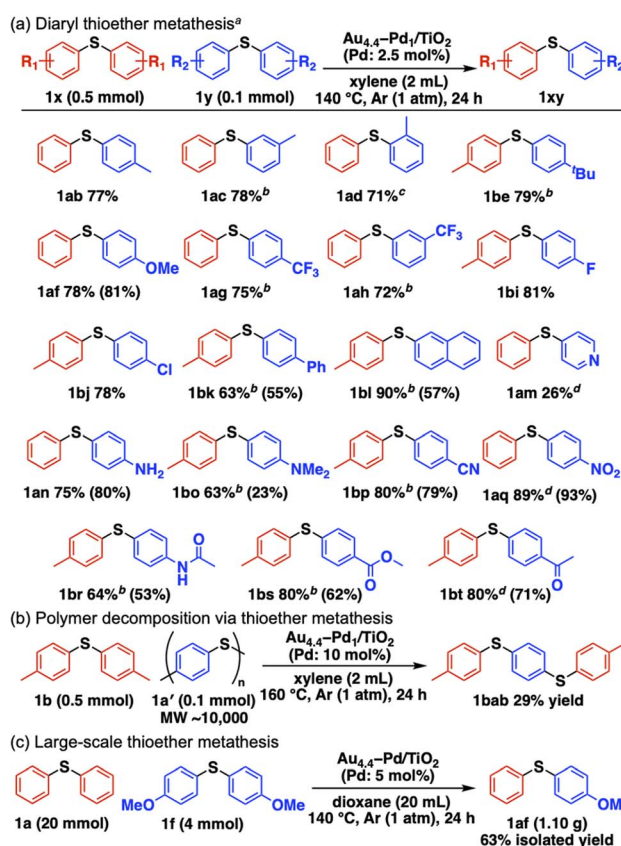
not improve the **1ab** yield (Table 1, entries 6 and 7), indicating that Au–Pd alloy formation is essential for the present C–S bond metathesis. After optimizing the supports (Table S4†), solvents (Table S5†), reaction temperatures (Table S6†), and **1a**/**1b** ratio (Table S7†), **1ab** was efficiently produced in 77% yield (Table 1, entry 8).

The C–S bond metathesis of **1a** and **1b** immediately ceased after hot filtration of $Au_{4.4}$–Pd_1/TiO_2 (Fig. S3†), and inductively coupled plasma-atomic emission spectroscopy (ICP-AES) detected almost zero Pd and Au species in the filtrate (Pd: below the detection limit, Au: 0.004% of the Au used in the reaction). Therefore, the observed catalysis was truly heterogeneous. Although the catalyst could be regenerated via calcination in an air followed by reduction with $NaBH_4$ and reused twice without significant loss of the final yield (Fig. S4†), the final **1ab** yield dropped at the 4th use. The average size of Au–Pd nanoparticles in the $Au_{4.4}$–Pd_1/TiO_2 after the 1st use observed by HAADF-STEM ($d = 3.70$ nm, $\sigma = 1.12$ nm) was a little larger than that of the fresh catalyst ($d = 3.05$ nm, $\sigma = 0.77$ nm) (Fig. 1c, d, and S5†), and a new peak assigned to Au(111) appeared in the XRD pattern of the catalyst after the 4th reuse (Fig. S6†),

Table 1 Effect of catalysts on the metathesis of **1a** and **1b**[a]

Entry	Catalyst	Conversion (%)		Yield (%)
		1a	**1b**	**1ab**
1	Pd_1/TiO_2	9	11	1
2	$Au_{0.7}$–Pd_1/TiO_2	9	20	11
3	$Au_{1.4}$–Pd_1/TiO_2	14	36	25
4	$Au_{3.0}$–Pd_1/TiO_2	19	62	52
5	$Au_{4.4}$–Pd_1/TiO_2	18	66	55
6[b]	$Au_{1.6}/TiO_2$	10	8	<1
7[b]	$Pd_1/TiO_2 + Au_{1.6}/TiO_2$	<1	3	3
8[c]	$Au_{4.4}$–Pd_1/TiO_2	21	84	77

[a] Conditions: **1a** (0.5 mmol), **1b** (0.1 mmol), catalyst (Pd: 2.5 mol%), xylene (2 mL), 120 °C, 3 h, Ar (1 atm). Conversions and yields were determined by GC. [b] $Au_{1.6}/TiO_2$ (Au: 4.0 mol%). [c] 140 °C, 24 h.

Scheme 2 Substrate scope. [a](a) Diaryl thioether metathesis. [a]Conditions: **1x** (0.5 mmol), **1y** (0.1 mmol), $Au_{4.4}$–Pd_1/TiO_2 (Pd: 2.5 mol%), xylene (2 mL), 140 °C, 24 h, Ar (1 atm). Yields were determined by GC. Values in parentheses are isolated yields. [b]$Au_{4.4}$–Pd_1/TiO_2 (Pd: 5 mol%). [c]$Au_{4.4}$–Pd_1/TiO_2 (Pd: 10 mol%). [d]$Au_{2.6}$–Pd_1/HAP (Pd: 10 mol%). (b) Polymer decomposition via thioether metathesis. Conditions are indicated in the scheme. (c) Large-scale thioether metathesis. Conditions are indicated in the scheme.
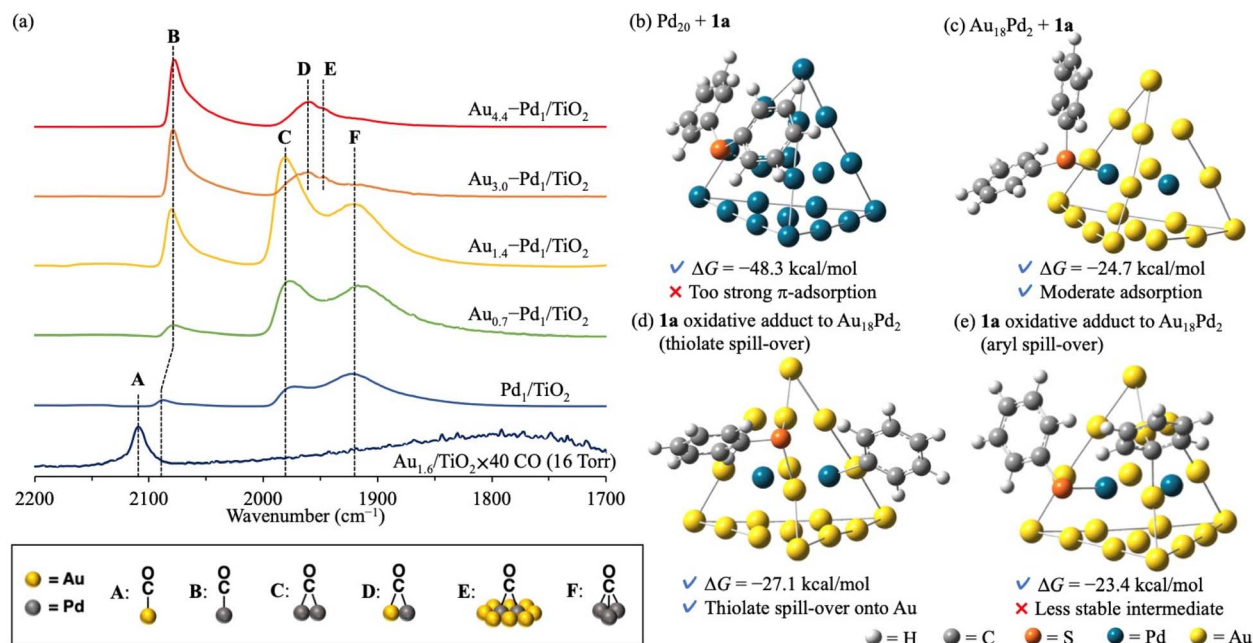
Fig. 2 Characterization of Au–Pd alloy nanoparticle catalysts and DFT calculations of **1a** adsorption using Pd_{20} and $Au_{18}Pd_2$ cluster models: (a) CO-DRIFT spectra of $Au_{1.6}/TiO_2$, Pd_1/TiO_2, and Au_x–Pd_1/TiO_2; optimized structures of **1a** adsorbed on (b) Pd_{20} and (c) $Au_{18}Pd_2$; optimized structures of **1a** oxidative adduct on (d) $Au_{18}Pd_2$ (thiolate spill-over to Au) and (e) $Au_{18}Pd_2$ (aryl spill-over to Au).

indicating that the aggregation of Au–Pd nanoparticles is one reason for the deactivation of the catalytic activity.

Scheme 2a summarizes the substrate scope of $Au_{4.4}$–$Pd_1/$TiO$_2$-catalyzed C–S bond metathesis of diaryl thioethers.§ Symmetrical methyl-substituted thioethers at the *para*, *meta*, and *ortho* positions afforded the corresponding unsymmetrical thioethers in good yields (**1ab**–**1ad**). Other electron-donating groups, including 4-*tert*-butyl and 4-methoxy groups, also afforded their metathesis products (**1be**, **1af**). This system is applicable to thioether metathesis with electron-withdrawing trifluoromethyl groups (**1ag**, **1ah**) and halogenated thioethers with fluoro and chloro groups (**1bi**, **1bj**). 4-Biphenyl-, 2-naphthyl-, and 4-pyridyl-substituted thioethers also served as competent metathesis partners (**1bk**, **1bl**, **1am**). Thioethers with amino (**1an**), *N*,*N*-dimethylamino (**1bo**), cyano (**1bp**), nitro (**1aq**), acetamide (**1br**), methyl ester (**1bs**), and acetyl (**1bt**) functional groups were converted into the corresponding unsymmetrical thioethers without disrupting the functional groups. Moreover, commercial polyphenylene sulfide (PPS, **1a′**) decomposed into 1,4-bis[(4-methylphenyl)thio]benzene (**1bab**) *via* metathesis between **1a′** and **1b** in the presence of $Au_{4.4}$–Pd_1/TiO_2 (Scheme 2b). Gram-scale synthesis from **1a** and **1f** afforded the metathesis product **1af** (1.10 g, 63% isolated yield) (Scheme 2c).

The effect of alloying on the present C–S bond metathesis of thioethers was determined from diffuse reflectance infrared Fourier transform (CO-DRIFT) spectra of adsorbed CO on $Au_{1.6}/$TiO$_2$, Pd_1/TiO_2, and Au_x–Pd_1/TiO_2 (Fig. 2a). In the CO-DRIFT spectra of Pd_1/TiO_2, $Au_{0.7}$–Pd_1/TiO_2, and $Au_{1.4}$–Pd_1/TiO_2, which exhibited low catalytic activity for the C–S bond metathesis (Table 1, entries 1–3), three peaks around 2070, 1980, and 1920 cm^{-1} were observed assignable to linear (**B**), bridged (**C**), and

and three-fold (**F**) CO species on zero-valent Pd species, respectively.[9] In the CO-DRIFT spectra of $Au_{3.0}$–Pd_1/TiO_2 and $Au_{4.4}$–Pd_1/TiO_2 showing high catalytic activity (Table 1, entries 4 and 5), peaks **C** and **F** were absent while new peaks at 1950 and 1940 cm^{-1} were attributable to CO species bridged on Au and Pd species (**D**) and on Pd species surrounded by Au species (**E**), respectively.[9d] As the Pd and Au–Pd alloy nanoparticles were similarly sized (Fig. 1c, d and S7†) and the peak of the CO species on Pd did not shift with increasing Au/Pd ratio in Au_x–Pd_1/TiO_2 (Fig. 2a), we attributed the high catalytic activity of $Au_{4.4}$–Pd_1/TiO_2 to the diluted Pd ensembles rather than to the ligand effect.

Next, the ensemble effect on the present C–S bond metathesis was investigated through DFT calculations on Pd_{20} and $Au_{18}Pd_2$ cluster models. Referring to previous reports, we adopted Gaussian 16 (M06 functional with SDD basis sets for Au and Pd and 6-31G(d,p) basis sets for H, C, and S)[10] (see ESI for the calculation methods and model selection) (Fig. S8–S10).† The adsorption Gibbs energy of **1a** was calculated at the center site of the Pd_{20} or $Au_{18}Pd_2$ cluster model.¶ The adsorption Gibbs energy of **1a** on Pd_{20} is very high ($\Delta G = -48.3$ kcal mol^{-1}), indicating that the metathesis product cannot easily desorb and the reaction is strongly inhibited (Fig. 2b). In contrast, **1a** adsorbed on $Au_{18}Pd_2$ has a moderate ΔG(−24.7 kcal mol^{-1}) and the reaction can proceed (Fig. 2c). The optimized structure of **1a** on Pd_{20} clarifies strong π-adsorption between **1a** and the Pd_{20} facets, whereas **1a** on $Au_{18}Pd_2$ adheres *via* coordination of its S atom to the Pd center with almost no π-adsorption. Corroborating this finding, the natural-bond orbital charge of the phenyl group is higher in Pd_{20}-adsorbed **1a** than in free **1a**, probably due to π-back donation from the Pd species to the

phenyl rings of **1a**,[11] but is lower in Au$_{18}$Pd$_2$–adsorbed **1a** than in free **1a**, possibly due to σ-donation from the S atom to the Pd atom (Fig. S11†). Facilitated by the weak π-back donation ability of the Au species,[12] the Pd ensembles diluted with Au alloy changed the **1a** adsorption mode and lowered the adsorption energy to enable the reaction (Scheme 1d).‖ Moreover, as indicated in the optimized structure of **1a** oxidative adducts to Au$_{18}$Pd$_2$ (Fig. S12 and S13†), the thiolate species produced by thioether oxidative addition on Pd species can transfer to the Au species without forming very stable structures (Fig. 2d), whereas the **1a** oxidative adduct *via* aryl spill-over to Au species gives a slightly higher Δ*G* (Fig. 2e).¶ Considering the aforementioned indirect thioether metathesis on Pd complexes,[5] thiolate spill-over onto the Au species probably promotes the trans-metalation, enabling an efficient direct diaryl thioether metathesis with no additives (Scheme 1d).

Conclusions

In conclusion, we achieved the first heterogeneously catalyzed direct C–S bond metathesis of diaryl thioethers with a wide substrate scope and functional group tolerance using Au$_{4.4}$–Pd$_1$/TiO$_2$. Catalyst characterization and DFT calculations revealed the likely causes of the high catalytic activity of Au$_{4.4}$–Pd$_1$/TiO$_2$: moderate adsorption energy of thioethers on the Au–Pd alloy nanoparticles (conferred by diluted Pd ensembles) and thiolate spillover onto Au species (which promotes subsequent trans-metalation). These findings are anticipated to guide the development of novel molecular transformations using multimetallic catalysts, especially by harnessing metal ensembles.

Data availability

The data (experimental procedures and characterization data) that support this article is available within the article and its ESI.†

Author contributions

T. Yatabe and K. Y. conceived and supervised the project. T. M. performed most of the experiments. T. Yabe performed the XAFS measurements. All authors contributed to data analysis and discussed the results. T. M. and T. Yatabe wrote the manuscript with feedback from K. Y. and T. Yabe.

Conflicts of interest

There are no conflicts to declare.

Acknowledgements

Notes and references

‡ Previously, we reported slight thioether metathesis between **1a** and **1b** in the presence of a hydroxyapatite-supported mono-metallic Pd nanoparticle catalyst[8] but under very different reaction conditions, using much more catalyst (Pd: 20 mol%) at a higher reaction temperature (160 °C) for 24 h.

§ As for the products that are difficult to be isolated by column chromatography, GC charts after the reaction can be found in Fig. S14.†

¶ The other adsorption sites are discussed in detail in the ESI.†

‖ Previously we identified *in situ* formed Pd nanoclusters as the active species of diaryl thioether metathesis.[7] In that case, π-adsorption of diaryl thioethers on Pd nanoclusters was probably suppressed by moderate steric hindrance of the PCy$_3$ ligand, enabling the metathesis to proceed.

1 (*a*) F. Gao and D. W. Goodman, *Chem. Soc. Rev.*, 2012, **41**, 8009; (*b*) H. Li, K. Shin and G. Henkelman, *J. Chem. Phys.*, 2018, **149**, 174705; (*c*) P. Liu and J. K. Nørskov, *Phys. Chem. Chem. Phys.*, 2001, **3**, 3814.

2 H. Ishikawa, S. Yamaguchi, A. Nakata, K. Nakajima, S. Yamazoe, J. Yamasaki, T. Mizugaki and T. Mitsudome, *JACS Au*, 2022, **2**, 419.

3 M. T. Greiner, T. E. Jones, S. Beeg, L. Zwiener, M. Scherzer, F. Girgsdies, S. Piccinin, M. Armbrüster, A. Knop-Gericke and R. Schlögl, *Nat. Chem.*, 2018, **10**, 1008.

4 (*a*) C.-F. Lee, Y.-C. Liu and S. S. Badsara, *Chem.–Asian J.*, 2014, **9**, 706; (*b*) K. L. Dunbar, D. H. Scharf, A. Litomska and C. Hertweck, *Chem. Rev.*, 2017, **117**, 5521; (*c*) E. A. Ilardi, E. Vitaku and J. T. Njardarson, *J. Med. Chem.*, 2014, **57**, 2832; (*d*) J. Lou, Q. Wang, P. Wu, H. Wang, Y.-G. Zhou and Z. Yu, *Chem. Soc. Rev.*, 2020, **49**, 4307. For the reviews of synthesis of thioethers, see; (*e*) P. Chauhan, S. Mahajan and D. Enders, *Chem. Rev.*, 2014, **114**, 8807; (*f*) T. Kondo and T. Mitsudo, *Chem. Rev.*, 2000, **100**, 3205; (*g*) S. V. Ley and A. W. Thomas, *Angew. Chem., Int. Ed.*, 2003, **42**, 5400.

5 (*a*) Z. Lian, B. N. Bhawal, P. Yu and B. Morandi, *Science*, 2017, **356**, 1059; (*b*) M. A. Rivero-Crespo, G. Toupalas and B. Morandi, *J. Am. Chem. Soc.*, 2021, **143**, 21331; (*c*) B. N. Bhawal and B. Morandi, *Angew. Chem., Int. Ed.*, 2019, **58**, 10074.

6 B. Mouhsine, M. Norlöff, J. Ghouilem, A. Sallustrau, F. Taran and D. Audisio, *J. Am. Chem. Soc.*, 2024, **146**, 8343.

7 T. Matsuyama, T. Yatabe, T. Yabe and K. Yamaguchi, *Catal. Sci. Technol.*, 2024, **14**, 76.

8 T. Matsuyama, T. Yatabe and K. Yamaguchi, *Org. Biomol. Chem.*, 2024, **22**, 579.

9 (*a*) T. Matsuyama, T. Yatabe, T. Yabe and K. Yamaguchi, *ACS Catal.*, 2022, **12**, 13600; (*b*) C.-W. Yi, K. Luo, T. Wei and D. W. Goodman, *J. Phys. Chem. B*, 2005, **109**, 18535; (*c*) X. Xu and D. W. Goodman, *J. Phys. Chem.*, 1993, **97**, 7711; (*d*) B. Zhu, G. Thrimurthulu, L. Delannoy, C. Louis,

C. Mottet, J. Creuze, B. Legrand and H. Guesmi, *J. Catal.*, 2013, **308**, 272.

10 (*a*) R. N. Dhital, C. Kamonsatikul, E. Somsook, K. Bobuatong, M. Ehara, S. Karanjit and H. Sakurai, *J. Am. Chem. Soc.*, 2012, **134**, 20250; (*b*) X.-F. Lang, P.-G. Yin, T.-T. You and L. Guo, *ChemPhysChem*, 2012, **13**, 237; (*c*) R. Miyazaki, X. Jin, D. Yoshii, T. Yatabe, T. Yabe, N. Mizuno, K. Yamaguchi and J. Hasegawa, *Catal. Sci. Technol.*, 2021, **11**, 3333; (*d*) D. Takei, T. Yatabe, T. Yabe, R. Miyazaki, J. Hasegawa and K. Yamaguchi, *JACS Au*, 2022, **2**, 394.

11 T. Wang, Y. Xu, J. Yang, X. Ju, W. Ding and Y. Zhu, *ChemCatChem*, 2019, **11**, 3770.

12 (*a*) L. Ouyang, G.-J. Da, P.-F. Tian, T.-Y. Chen, G.-D. Liang, J. Xu and Y.-F. Han, *J. Catal.*, 2014, **311**, 129; (*b*) J. H. Lee, J. Cho, M. Jeon, M. Ridwan, H. S. Park, S. H. Choi, S. W. Nam, J. Han, T.-H. Lim, H. C. Ham and C. W. Yoon, *J. Mater. Chem. A*, 2016, **4**, 14141; (*c*) W. Wang, R. J. Lewis, B. Lu, Q. Wang, G. W. Hutchings, J. Xu and F. Deng, *ACS Catal.*, 2024, **14**, 2522.